HHS Public Access

Author manuscript

Cytotherapy. Author manuscript; available in PMC 2024 August 01.

Published in final edited form as:

Cytotherapy. 2024 August ; 26(8): 858–868. doi:10.1016/j.jcyt.2024.03.006.

Human platelet lysate enhances *in vivo* activity of CAR-Vδ2 T cells by reducing cellular senescence and apoptosis

Feiyan Mo[1,2], **Chiou-Tsun Tsai**[1], **Rong Zheng**[3,4], **Chonghui Cheng**[3,4], **Helen E Heslop**[1,2], **Malcolm K Brenner**[1,2], **Maksim Mamonkin**[1,2], **Norihiro Watanabe**[1,#]

[1]Center for Cell and Gene Therapy, Baylor College of Medicine, Texas Children's Hospital and Houston Methodist Hospital, Houston, TX, USA

[2]Graduate Program in Translational Biology and Molecular Medicine, Baylor College of Medicine, Houston, TX, USA

[3]Department of Molecular and Human Genetics, Lester & Sue Breast Center, Baylor College of Medicine, Houston, TX, USA

[4]Graduate Program in Integrative Molecular and Biomedical Sciences, Baylor College of Medicine, Houston, TX, USA

Abstract

Vγ9Vδ2 T cells are an attractive cell platform for the off-the-shelf cancer immunotherapy due to their lack of alloreactivity and inherent multi-pronged cytotoxicity, which could be further amplified with chimeric antigen receptors (CARs). In this study, we sought to enhance the *in vivo* longevity of CAR-Vδ2 T cells by modulating *ex vivo* manufacturing conditions and selecting an optimal CAR costimulatory domain. Specifically, we compared the anti-tumor activity of Vδ2 T cells expressing anti-CD19 CARs with costimulatory endodomains derived from CD28, 4–1BB or CD27 and generated in either standard fetal bovine serum (FBS)- or human platelet lysate (HPL)-supplemented medium. We found that HPL supported greater expansion of CAR-Vδ2 T cells with comparable *in vitro* cytotoxicity and cytokine secretion to FBS-expanded CAR-Vδ2 T cells. HPL-expanded CAR-Vδ2 T cells showed enhanced *in vivo* anti-tumor activity with longer T cell persistence compared to FBS counterparts, with 4–1BB costimulated CAR showing the greatest activity. Mechanistically, HPL-expanded CAR Vδ2 T cells exhibited reduced apoptosis and senescence transcriptional pathways compared to FBS-expanded CAR-Vδ2 T cells and increased telomerase activity. This study supports enhancement of therapeutic potency of CAR-Vδ2 T cells through a manufacturing improvement.

[#] **Correspondence should be addressed to:** Norihiro Watanabe, Ph.D., Baylor College of Medicine, 1102 Bates Ave Ste 1770.18, Houston, TX 77030, nwatanab@bcm.edu.

Present address:

The current affiliation for F.M. is Department of Medicine, University of Pennsylvania Perelman School of Medicine, Philadelphia, PA.

Author contributions

F.M. and C.T.T. performed experiments, analyzed data. R.Z. and C.C. performed the analysis of the RNA-seq data. H.E.H, M.K.B. and M.M. advised on the study, critically reviewed manuscript. N.W. conceptualized and directed the study, designed and performed experiments, analyzed and interpreted data, and wrote the manuscript. All authors reviewed and edited the manuscript.

Keywords

Vδ2 T cells; chimeric antigen receptor; Manufacture; Human platelet lysate; apoptosis; cell senescence

Background

Allogeneic off-the-shelf (OTS) therapeutic cells have several advantages over conventional autologous therapies as they offer an immediate treatment at a lower cost and with minimal inter-product heterogeneity. OTS cell products must lack host alloreactivity which requires either additional genetic manipulations in donor-derived αβT cells or utilizing naturally non-alloreactive cell populations. Vγ9Vδ2 T cells are one such subset with inherent lack of alloreactivity due to the expression of a T cell receptor (TCR) that recognizes a structural change of the BTN2A1-BTN3A1 molecules in an MHC-independent manner.[1,2] This structural alteration is often found on the cell surface of cancer cells due to the dysregulation of the mevalonate pathway. Apart from the TCR, Vγ9Vδ2 T cells can directly kill tumor cells via NKG2D,[3] the ligand for MHC class I polypeptide-related sequence A and B (MICA/B) and UL16 binding proteins (ULBPs) expressed on many tumor cells. Vδ2 T cells also mediate antibody-dependent cell cytotoxicity via the Fc receptor CD16 (FcγRIII) expressed on a subpopulation of Vδ2 T cells.[4] Although Vδ2 T cells are a small subset of T cells found in peripheral blood, this cell population can be easily expanded *ex vivo* by treating peripheral blood mononuclear cells (PBMCs) with Zoledronic acid (Zol), which has been used in clinic to treat osteoporosis.[5] Because of their inherent multi-pronged cytotoxicity and ease of manufacture, adoptive transfer of *ex vivo* expanded Vδ2 T cells has been used to treat multiple cancers; however, clinical responses in several studies have been underwhelming,[6] prompting efforts to boost anti-tumor activity of Vδ2 T cells through arming with chimeric antigen receptors (CARs) and other receptors.[7]

In the present study, we aimed to further enhance the efficacy of CAR-modified Vδ2 T cells by modifying their *ex vivo* manufacturing to boost clinical potency of therapeutic cells. We have previously shown that substituting human platelet lysate (HPL) for fetal bovine serum (FBS) or human AB serum (ABS) in culture medium enhances the *in vivo* longevity of CAR-αβT cells by maintaining a less-differentiated memory phenotype such as naïve-like and central memory T cells.[8] We hypothesized that this strategy could be applied to enhance *in vivo* efficacy of CAR-Vδ2 T cells. In addition, we compared the function of CAR costimulatory domains for Vδ2 T cells that had been expanded in different medium formulations, and we evaluated their activity against tumor *in vitro* and *in vivo*. In this report, we demonstrate that the *in vivo* functionality of CAR-Vδ2 T cells is highly affected by medium formulations and the choice of CAR costimulation.

Materials and Methods

Donors and cell lines

Peripheral blood mononuclear cells (PBMCs) were obtained from healthy volunteers after informed consent on protocols approved by the Baylor College of Medicine Institutional

Review Board (H-45017). 293T (human embryonic kidney cell line), NALM6 (pre-B cell acute lymphoblastic leukemia cell line) and Raji (Burkitt lymphoma cell line) were obtained from the American Type Culture Collection (Rockville, MD). 293T cells were maintained in DMEM medium (Gibco BRL Life Technologies, Inc., Gaithersburg, MD) whereas NALM6 and Raji cells were maintained in RPMI-1640 medium (GE Healthcare Life Sciences, Pittsburgh, PA). All media were supplemented with 10% heat-inactivated FBS (Gibco BRL Life Technologies, Inc.) and 2 mM L-GlutaMAX (Gibco BRL Life Technologies, Inc.). Cells were maintained in a humidified atmosphere containing 5% carbon dioxide (CO2) at 37 °C and have been routinely tested for Mycoplasma.

Generation of retroviral constructs and retrovirus production

Second generation CAR construct targeting CD19 with CD28z signaling domain was previously generated.[8] In brief, the CAR construct is composed of an scFv domain (clone FMC63) followed by IgG2-derived hinge and CH3 spacer with CD28 transmembrane/costimulatory and CD3z signaling domain. In this study, FLAG tag (DYKDDDDK) was inserted between V_L and V_H regions with G_4S linker before and after to facilitate detection of surface CAR expression by utilizing In-Fusion Snap Assembly kit (Takara Bio USA, Inc., San Jose, CA). Further, CD28 costimulatory domain was replaced to 4–1BB and CD27 costimulatory domains with this method. The γ-retroviral vector encoding green fluorescent protein /Firefly luciferase fusion protein (GFP/FFLuc) and the retroviral supernatant was generated as previously described.[9]

Generation of CAR-modified Vδ2 T cells and gene-modified cell lines

CAR-Vδ2 T cells were generated/maintained in CTL media [50% RPMI-1640, 50% Clicks medium (Irvine Scientific, Inc., Santa Ana, CA) and 2 mM L-GlutaMAX)] supplemented with 10% of either FBS, ABS (Valley Biomedical, Winchester, Virginia) or HPL (nLiven PR™; Sexton Biotechnologies, BioLife Solutions Inc., Bothell, WA). To generate CAR-Vδ2 T cells, PBMCs (10^6 cells/mL) were first stimulated with 1 μM of Zoledronate (Zoledronic acid; SML0223, Sigma-Aldrich, St. Louis, MO) in the presence of 100 U/mL of recombinant human IL-2 (NIH, Bethesda, VA). Five days later, γδT cells were negatively isolated by using TCRγ/δ+ T Cell Isolation Kit (Miltenyi Biotec Inc., San Diego, CA). For CAR retrovirus transduction, retroviral supernatant was plated in a non-tissue culture-treated 24-well plate pre-coated with Retronectin reagent (Takara Bio USA, Inc.), and centrifuged at 2,000 xg for 2 hrs. After removal of the supernatant, γδTCR(+)-isolated cells (0.1×10^6/mL) were resuspended in each medium supplemented with IL-2 (100 U/mL) and 2 mL was added to each virus loaded well, which was subsequently spun at 800 xg for 5 min, and then transferred to a 37 °C, 5% CO2 incubator. Subsequently, cells were split and fed every 2–3 days with fresh media plus IL-2 (100 U/mL). On day 14 post-transduction, residual αβTCR(+) cells were depleted from cultures by using EasySep™ Human TCR Alpha/Beta Depletion Kit (StemCell Technologies, Vancouver, Canada). Cells were frozen and then thawed for functional assessment. To generate tumor cell lines overexpressing GFP/FFLuc, we used the same protocol as described above and isolated the GFP positive fraction using a cell sorter (SH800S, Sony Biotechnology, San Jose, CA).

While CAR-Vδ2 T cells were generated in CTL medium containing different serum supplements, all *in vitro* functional assays were performed in CTL medium supplemented with 10% FBS.

Flow cytometry

Cells were stained with fluorochrome-conjugated antibodies for 20 min at 4 °C. All samples were acquired on a Gallios Flow Cytometer (Beckman Coulter Life Sciences, Indianapolis, IN) or Cytek Northern Lights (Cytek Biosciences, Inc., Fremont, CA), and data was analyzed using Kaluza 2.1 Flow Analysis Software (Beckman Coulter Life Sciences). Antibodies used in this study are listed in supplemental table S1.

Degranulation assay and intracellular cytokine staining

Freshly thawed 0.2×10^6 CAR-Vδ2 T cells were cocultured with 0.2×10^6 either NALM6-GFP/FFLuc or Raji-GFP/FFLuc cells in 200 μL in the presence of Monensin (BD GolgiStop, BD Biosciences, San Jose, CA) and CD107a-APC antibody (clone H4A3/641581) for 4 hrs. After the incubation, cells were stained for cell surface markers and BD Horizon Fixable Viability Stain 700 (BD Biosciences). Stained cells were then fixed and permeabilized with BD Cytofix/Cytoperm (BD Biosciences) according to the manufacturer's protocol. Cytokines IFN-γ, TNF-α, IL-2, and IL-17A were stained and analyzed by flow cytometry.

Cytokine quantification

To measure cytokine production, freshly thawed 0.2×10^6 CAR-Vδ2 T cells were cocultured with 0.2×10^6 target cells in 200 μL of medium in a single well of a flat-bottom 96-well plate for 24 hrs. Supernatants were collected and stored at −80 °C. Cytokine levels were analyzed using MILLIPLEX MAP Kit (Merck Millipore, Billerica, MA), according to manufacturer's instructions.

Coculture experiments

In the short-term coculture experiments, freshly thawed 5,000 or 10,000 CAR(+) CAR-Vδ2 T cells were cocultured with 20,000 GFP/FFLuc(+) target cell lines in 200 μL in the presence of 50 U/mL of IL-2 in one well of 96-well flat-bottom plates. Cells were harvested and analyzed by flow cytometry on day 3. In the long-term coculture experiments, freshly thawed 10,000 CAR(+) Vδ2 T cells were cocultured with 20,000 GFP/FFLuc(+) target cell lines in 200 μL in the absence of exogenous cytokine in one well of 96-well flat-bottom plates. Cells were harvested, stained, and analyzed by flow cytometry on days 0, 3, 6 and 9. To quantify cell counts by flow cytometry, 10 μL/sample of CountBright Absolute Counting Beads (Thermo Fisher Scientific, Invitrogen, Grand Island, NY, USA) was added, and 7-AAD (BD Biosciences) was added to exclude dead cells. Acquisition was halted at 1,000 beads.

In vivo study

Breeder pairs of NOD.Cg-Prkdc^{scid} Il2rg^{tm1Wjl}/SzJ mice (NSG mice; Strain no. 005557) were purchased from the Jackson Laboratory and bred in the Baylor College of Medicine

animal facility. Both female and male littermates (aged 8–12 weeks) were used for experiments. All animal experiments were conducted in compliance with the Baylor College of Medicine Institutional Animal Care and Use Committee (IACUC) (protocol no. AN-4758). To evaluate the *in vivo* anti-tumor effect of CAR-Vδ2 T cells, 0.5×10^6 NALM6-GFP/FFLuc cells were injected into NSG mice intravenously. Three days later, tumor-bearing mice were grouped based on average tumor bioluminescence evaluated by injecting mice intraperitoneally with 100 μL D-luciferin (30 mg/mL; PerkinElmer, Waltham, MA, USA) followed by bioluminescence imaging using an IVIS Lumina II imaging system (Caliper Life Sciences, Hopkinton, MA, USA). Freshly thawed 4 or 10×10^6 CAR-Vδ2 T cells were injected into mouse intravenously. After treatment, mice were housed with their original cage mates, to minimize potential confounders such as the order of measurements or animal location. Tumor cell growth was evaluated by bioluminescence imaging and analyzed by Living Image software (Caliper Life Sciences). To quantify T cells in the mouse peripheral blood, 50 μL of blood obtained by tail vein bleeding was stained with CD3, Vδ2TCR, FLAG, and CD45, then treated with RBC Lysis Buffer (BioLegend, San Diego, CA) to lyse red blood cells. CD45(+)CD3(+)Vδ2TCR(+)FLAG(+) cells were counted by flow cytometry using CountBright Absolute Counting Beads. These studies included a total 147 mice (male: 72, female: 75).

RNA sequencing and data analysis

CD19.CAR (4–1BB)-modified Vδ2 T cells were generated in either FBS- or HPL-supplemented medium from four different donors. On day 7 post-transduction, CAR(+) cells were stained with FLAG-PE/Cy7 and anti-Cy7-microbeads (Miltenyi Biotec Inc.), and isolated with MACS system. On day 14 post-transduction, Vδ2TCR(+) cells were sorted using a cell sorter (SH800S, Sony Biotechnology) before total RNA extraction. Total RNA was extracted from isolated/purified CAR(+)Vδ2(+) T cells using the RNeasy plus Mini kit (QIAGEN, Valencia, CA). Preparation of mRNA library and next generation sequencing were performed by Genewiz (Azenta Life Sciences; South Plainfield, NJ) using Illumina NovaSeq (read length: 2×150 bp, number of reads per sample: 20–30 million).

RNA-seq reads were aligned to the human genome (GRCh38, primary assembly) and transcriptome (Gencode version 38 primary assembly gene annotation) using STAR v2.7.9a with the following non-standard parameters --outSAMstrandField intronMotif -- outFilterType BySJout --outFilterMultimapNmax 1 --alignSJoverhangMin 8 --alignSJDBoverhangMin 3 --alignEndsType EndToEnd. Only uniquely aligned reads were retained for downstream analysis.

Differential gene expression analysis was performed by counting reads over genes from the same annotation as alignment using featureCounts version 1.5.0 with the following non-default parameters -s 0 -a. Differential gene expression analysis was conducted using DESeq2 performed on genes with at least 5 counts present in at least half of the samples. Significantly regulated genes were defined as genes with an $|\log2FC| > 1$ and FDR < 0.05.

log2-transformed counts per million (CPM) normalization and the trimmed mean of M-values (TMM) adjustment were applied to raw count matrix, and variances of normalized gene expression across samples were then calculated and used for the ranking of all

adequately expressed genes in unsupervised hierarchical clustering. The unsupervised clustering heatmaps were produced using Euclidean clustering.

Gene Set Enrichment Analysis was performed on GSEA software (v4.2.3) from Broad institute.[10,11] We utilized the following Molecular Signatures Database (MSigDB)[12,13]; h.all.v2023.1.Hs.symbols.gmt, c2.cp.reactome.v2023.1.Hs.symbols.gmt, c2.cp.kegg.v2023.1.Hs.symbols.gmt, c5.go.v2023.1.Hs.symbols.gmt.

Telomeric repeat amplification protocol (TRAP)

Endogenous telomerase activity from CAR-Vδ2 T cells was detected using the TRAPese® Telomerase Detection Kit (Cat No. S7700, MilliporeSigma™ Chemicon™) under the manufacturer's instruction. Briefly, 3×10^5 purified CAR-Vδ2 T cells were lysed with 60 μL 1x CHAPs lysis buffer for 30 min on ice, and after 12,000 xg centrifuge, 2 μL lysates were added into a 48 μL reaction mixture [5 μL 10x TRAP reaction buffer, 1 μL 10 mM dNTP, 1 μL TS primers, 1 μL TRAP primer mix, and 1 unit DNA Polymerase (Q5® High-Fidelity, NEB)], and subjected to a two- step thermal reaction which involved 30°C incubation for 1 hour, followed by 98°C for 3 min, 31 PCR cycles of 98°C for 10 sec, 59°C for 10 sec and 72°C for 30 sec. PCR products were separated and analyzed by 12% non-denaturing 0.5x Tris-borate-ETDA PAGE electrophoresis, and subsequently stained with ethidium bromide for 30 min. The signal was detected and displayed through Gel Doc™ EZ Imager (Bio-Rad).

Statistical analysis

Statistical analysis was performed using Graphpad Prism 7 software (GraphPad Software, Inc., La Jolla, CA). The statistical analysis used in each experiment is described in the figure legend.

Results

Human platelet lysate (HPL) supports CAR-Vδ2 T cell expansion

To generate CAR-Vδ2 T cells, we stimulated PBMCs with Zol (1 μM) and IL-2 (100 U/mL) in either 10%HPL-supplemented medium or 10%FBS-supplemented medium. On day 5, γδTCR(+) cells were negatively isolated to enrich Vδ2 T cells, then transduced with a CAR construct with the different costimulatory domains. In this study, we utilized a model CAR targeting CD19 (CD19.CAR) which is widely used in preclinical and clinical studies. We expanded CAR-Vδ2 T cells for another 14 days and cryopreserved them before evaluating their function (figure 1A). At culture completion, we found higher cell expansion in the HPL-cultured condition compared to the FBS-cultured condition, especially in cells transduced with the CD19.CAR regardless of the CAR costimulatory domain (figure 1B). Most of these expanded cells were positive for Vδ2TCR; small populations of Vδ1TCR(+), αβTCR(+), and CD56(+)CD3(−) cells were also found across culture conditions in both non-transduced (NT) and CAR-transduced products regardless of the exact CAR construct (supplemental figures S1A and S1B). In addition, CAR expression levels on Vδ2 T cells were comparable across CAR constructs and culture conditions (figure 1C), indicating HPL did not interfere with gammaretroviral transduction. We next

evaluated the cell surface phenotype of CAR-Vδ2 T cells. In contrast to our previous observations on CAR-αβT cells, there was no difference in memory phenotype (defined by CD27 and CD45RA expression) between the two culture conditions and most CAR-Vδ2 T cells showed an effector memory phenotype [CD27(−)CD45RA(−)] (figure 1D and supplemental figure S1C). However, HPL-expanded CAR-Vδ2 T cells had higher percentage of CD56(−)CD16(−) and CD25(+)CD71(+) subsets compared to FBS-expanded CAR-Vδ2 T cells (figure 1D and supplemental figure S1C). *Ex vivo* expanded Vδ2 T cells expressed high levels of NKG2D regardless of culture condition or CAR constructs (supplemental figure S1D). Thus, expanding CAR-Vδ2 T cells in HPL medium led to higher cell expansion with a distinct surface phenotypes compared to conventional FBS medium.

HPL- and FBS-expanded CAR-Vδ2 T cells show comparable effector function *in vitro*

We next evaluated and compared the function of each CAR-Vδ2 T cell product. To emulate clinical applications, we used freshly thawed CAR-Vδ2 T cells to set up *in vitro* functional assays. After 4hr coculture with CD19(+) NALM6 and Raji cell lines, HPL-expanded CAR-Vδ2 T cells showed comparable degranulation, as measured by CD107a (figure 2A and supplemental figure S2A), and cytokine production (figure 2B and supplemental figure S2B) compared to FBS-expanded CAR-Vδ2 T cells. HPL-expanded 4–1BB- and CD27-costimulated CD19.CAR-Vδ2 T cells secreted higher amounts of soluble FasL and Granzyme B, respectively, compared to their FBS counterparts (figure 2C). Notably, intracellular cytokine staining (supplemental figure S2C) and Luminex assay (data not shown) indicated that CAR-Vδ2 T cells generated in our protocol in either FBS- or HPL-supplemented media did not produce IL-17, a cytokine associated with pro-tumor activity.[14] To evaluate the cytotoxicity of CAR-Vδ2 T cells, we next performed 3-day *in vitro* coculture experiments in which CAR-Vδ2 T cells were cocultured with target cell lines-expressing green fluorescent protein (GFP) at 1:2 or 1:4 ratios in the presence of IL-2 (50 U/mL) added to support T cell survival. Cocultures were harvested on day 3 and residual target cells were evaluated by flow cytometry (figure 2D). In NALM6 cocultures, both FBS- and HPL-expanded CD19.CAR-Vδ2 T cells showed strong cytotoxicity at both 1:2 and 1:4 ratio (figure 2E, **top panels**). Of note, HPL-expanded Vδ2 T cells without CAR modification also killed the target cells, likely due to innate mechanisms of cytotoxicity in Vδ2 T cells. Similarly, both FBS- and HPL-expanded CD19.CAR-Vδ2 T cells showed significant cytotoxicity in coculture with Raji cells at the higher E:T ratios (1:2), and to a lesser extent at the lower E:T ratios (1:4) (figure 2E, **bottom panels**). Overall, CD19.CAR-Vδ2 T cells generated in both FBS- and HPL-supplemented media showed potent *in vitro* anti-tumor effect against CD19(+) cell lines compared to unmodified Vδ2 T cells.

HPL-expanded CD19.CAR-Vδ2 T cells showed superior *in vivo* anti-tumor effect in a mouse xenograft model of B-ALL

Since we observed only minimal differences of *in vitro* functionality between CAR-Vδ2 T cells generated in different medium formulations and CAR endodomains, we investigated long-term functionality *in vivo.* To assess the *in vivo* anti-tumor effect of CD19.CAR-Vδ2 T cells generated in different conditions, we first engrafted mice with 0.5×10^6 NALM6-expressing GFP/firefly luciferase (FFLuc) by intravenous injection. Three days later, tumor-bearing mice were randomized and treated with a single injection of freshly

thawed CD19.CAR-Vδ2 T cells (10×10^6 CAR+ cells/mouse). We also administered IL-2 (2,000 U/mouse, twice/week) over 4 weeks and tracked tumor growth by IVIS imaging (figure 3A). Compared to controls (Tumor only), FBS-expanded CAR-Vδ2 T cells had minimal anti-tumor effect regardless of their CAR costimulatory domain (figure 3B) and we only observed transient, albeit statistically significant, anti-tumor activity on days 3 and 7 after T cell treatment (figure 3C). In contrast, HPL-expanded CD19.CAR-Vδ2 T cells had enhanced anti-tumor activity, greatest in mice receiving CARs containing the 4–1BB costimulatory domain (figures 3B and 3C). We also detected higher numbers of HPL-expanded CD19.CAR-Vδ2 T cells in peripheral blood compared to their FBS counterparts, with the highest numbers in recipients of CARs with the 4–1BB costimulatory domain (figure 3D). These differences translated to increased overall survival in mice treated with HPL-expanded CD19.CAR Vδ2 T cells with the 4–1BB costimulatory domain (figure 3E). We also compared single and double injections in the same xenograft model using a lower dose of CAR-Vδ2 T cells (4×10^6 cells/mouse) (supplemental figure S3A). Although the overall anti-tumor effect was weaker than that with the 10×10^6 CAR-Vδ2 T cell dose, HPL-expanded CAR-Vδ2 T cells delayed tumor growth and still outperformed their FBS counterparts (supplemental figure S3B), prolonging overall mouse survival (supplemental figure S3C). A second infusion of 4–1BB costimulated CD19.CAR-Vδ2 T cells resulted in a marginal but statistically significant extension of mouse survival (supplemental figure S3C), supporting a dose-dependent benefit of CAR-Vδ2 T cell treatment. Thus, CAR-Vδ2 T cells manufactured in either FBS- or HPL-supplemented medium produced comparable short-term *in vitro* functionality but HPL-expanded CAR-Vδ2 T cells had enhanced *in vivo* anti-tumor effect with prolonged T cell survival.

The gene signatures of HPL-expanded CAR-Vδ2 T cells suggest reduced sensitivity to apoptosis and cellular senescence compared to FBS-expanded CAR-Vδ2 T cells

We sought to identify the fundamental characteristics correlating with the improved *in vivo* anti-tumor activity of HPL-expanded CAR Vδ2 T cells by RNA sequencing of Vδ2 T cells expressing a 4–1BB costimulated CD19.CAR manufactured in either FBS- or HPL-supplemented media from four donors (figure 4A). We identified a total of 4,561 differentially expressed genes (DEGs) in the RNA extracted from FBS- versus HPL-expanded CD19.CAR Vδ2 T cells (supplemental figures S4A and S4B). Principal component analysis showed two distinct clusters between FBS- and HPL-expanded CAR-Vδ2 T cells with some donor-to-donor variability (figure 4B). Gene Set Enrichment Analysis (GSEA) with Hallmark molecular signatures database demonstrated that gene signatures related to cytokine signaling (green) and apoptosis (blue) were highly enriched in FBS-expanded CAR-Vδ2 T cells compared to HPL-expanded CAR-Vδ2 T cells (figure 4C and supplemental figure S4C). In addition, FBS-expanded CAR-Vδ2 T cells had a gene signature enriched for cell senescence (red) and cell senescence related pathways[15–17] (purple) based on both the Hallmark molecular signatures database (figure 4C) and the Reactome molecular signatures database (figure 4D). These data suggested that, compared to FBS-expanded CAR-Vδ2 T cells, HPL-expanded CAR-Vδ2 cells received less cytokine signaling at base line, resulting in a lower expression of apoptosis and cellular senescence-associated genes prior to antigen stimulation.

To validate these transcriptomic findings, we investigated the susceptibility of CAR-Vδ2 T cells to apoptosis, by coculturing them with tumor cells for 9 days in the absence of exogenous IL-2, thus removing a pro-survival signal and rendering Vδ2 T cells susceptible to apoptosis. HPL-expanded CAR-Vδ2 T cells showed improved survival compared with their FBS counterparts (figure 4E **left**), leading to improved anti-tumor activity (figure 4E **right**). We next investigated the cell senescence status of CAR-Vδ2 T cells by measuring T cell senescence markers CD57 and KLRG1. Consistent with the RNA-seq data, FBS-expanded CAR-Vδ2 T cells showed higher levels of both senescence makers compared to HPL-expanded CAR-Vδ2 T cells (figure 4F). Because cell senescence is inversely correlated with telomerase activity, we compared telomerase activity of FBS- and HPL-expanded CAR-Vδ2 T cells using a Telomeric Repeat Amplification Protocol (TRAP) assay. As shown in figure 4G, CAR-Vδ2 T cells generated in HPL showed longer telomeric repeats compared to FBS-expanded CAR-Vδ2 T cells, demonstrating higher telomerase activity of HPL-expanded CAR-Vδ2 T cells. Collectively, these results indicated that HPL supplementation reduced the susceptibility of CAR-Vδ2 T cells to apoptosis and improved telomerase activity, correlating with the reduced senescence and increased functional persistence of CAR-Vδ2 T cells *in vivo*.

HPL-expanded CAR-Vδ2 T cells outperformed human AB serum supplemented CAR-Vδ2 T cells

Although FBS has been widely used to expand various types of immune cells in preclinical and early clinical studies, human-derived supplements are less immunogenic and have minimal risk of carrying non-human pathogens. To investigate if non-human components in FBS are the main cause of differences between FBS- and HPL-expanded Vδ2 T cells, we conducted side-by-side functional comparison of Vδ2 T cells expressing a 4–1BB costimulated CD19.CAR manufactured in medium supplemented with FBS, HPL, or ABS. CAR-Vδ2 T cells were generated using the same procedure as shown in figure 1A. CAR-Vδ2 T cells expanded with ABS showed reduced expansion compared to the HPL condition (figure 5A) but a comparable percentage of the Vδ2 T cell fraction (figure 5B). However, we observed significantly higher CAR expression on Vδ2 T cells expanded in ABS (figure 5C). Surface phenotype and the expression of proliferation and senescence markers by CAR-Vδ2 T cells were similar between FBS and ABS conditions and distinct from HPL-expanded cells (figure 5D and supplemental figure S5A). We then compared the *in vivo* anti-tumor effect of CAR-Vδ2 T cells generated under different conditions in the NALM-6 xenograft model (figure 3A). After CAR-Vδ2 T cell injection, all CAR-Vδ2 T cells had a short-term anti-tumor effect against NALM6 targets *in vivo* (figure 5E and supplemental figure S5B), but the activity of HPL-expanded CAR-Vδ2 T cells was greatest (figure 5E and supplemental figure S5B). We also observed a higher number of peripheral blood CAR-Vδ2 T cells in mice treated with HPL-expanded CAR-Vδ2 T cells (figure 5F), which translated into better overall survival (figure 5G). These results from the side-by-side comparison demonstrated that CAR-Vδ2 T cells generated in HPL-supplemented medium have more potent *in vivo* anti-tumor activity compared to media supplemented with FBS or ABS.

Discussion

We have shown that HPL-supplemented culture medium supports the generation of CAR-modified Vδ2 T cells with enhanced *in vivo* anti-tumor activity compared to conventional serum supplements such as FBS and ABS. HPL supplementation elicits higher *ex vivo* expansion of CAR-Vδ2 T cells with reduced cell death, cellular senescence, and enhanced *in vivo* functionality.

Clinical trials with cancer patients treated with aminobisphosphonates such as pamidronate (PAM) and zoledronate (Zol) to stimulate/expand Vδ2 T cells *in vivo* or with infusions of *ex vivo* expanded Vδ2 T cells showed disappointing clinical responses.[6] Therefore, multiple studies have explored approaches to increase the potency of Vδ2 T cells. One strategy is to modify Vδ2 T cells to express a CAR[18] (by either virus transduction, transposon/transposase or RNA transfection), a co-stimulatory CAR,[19] or to produce a bispecific T cell engagers (BiTE).[20,21] These modifications enhanced the functionality of Vδ2 T cells but often required multiple injections of high numbers of the engineered Vδ2 T cells to induce significant anti-tumor response,[22–25] reflecting short *in vivo* persistence of Vδ2 T cells.[26]

Clinical studies with CD19.CAR-modified αβT cells showed that functional persistence post-infusion correlated with superior outcomes.[27,28] We have previously shown that expansion of CAR-αβT cells in HPL-supplemented medium improved their *in vivo* persistence by maintaining a less-differentiated memory phenotype during manufacture.[8] We hypothesized that the same approach can be used to improve phenotype and cell composition of CAR-Vδ2 T cells. In contrast to αβT cells, we observed no change in memory phenotype of Vδ2 T cells generated with HPL. However, HPL expansion reduced apoptosis and cellular senescence which correlated with a significantly improved persistence and anti-tumor activity of CAR-Vδ2 T cells. Of the three costimulatory endodomains tested (CD28, 4–1BB, CD27), 4–1BB costimulated CARs enabled longest persistence of CAR-Vδ2 T cells *in vivo*, consistent with multiple CAR-αβT cell studies.[29,30]

While cell senescence is generally associated with aging, there is a growing interest in preventing senescence to enhance the efficacy of adoptively transferred therapeutic cells. T cell senescence has been studied largely in αβT cells where senescent cells share some characteristics with terminally differentiated T cells such as loss of CCR7, CD27 and CD28 expression with concomitant upregulation of CD57, KLRG1, and CD45RA.[31] Another key feature of senescent T cells is a loss of telomerase activity resulting in poor proliferation.[32] Our results demonstrated that FBS-expanded CAR-Vδ2 T cells showed enhanced T cell senescence features compared with HPL-expanded CAR-Vδ2 T cells. In addition, RNA sequencing and GSEA revealed that FBS-expanded CAR-Vδ2 T cells exhibited gene signatures associated with cytokine signaling such as IFN-α, IFN-γ, TNF-α, IL-6/JAK-STAT3 and IL-2/STAT5 signaling (figure 4C and supplemental figure S4C) by some of which (e.g, IFN-α[33,34] and IL-6/STAT3[35,36]) promote cell senescence. Furthermore, the contribution of TNF-α signaling to activation-induced cell death has been shown previously[37,38]. Overall, these results suggest that enhanced cytokine signaling facilitates cell senescence and increases susceptivity to apoptosis in FBS-expanded CAR-Vδ2 T cells, diminishing their anti-tumor efficiency. Conversely, the enhanced *in vivo* anti-tumor effect

of HPL-expanded CAR-Vδ2 T cells is consistent with the observed attenuation of those pathways during manufacture process. However, factor(s) contained in HPL that confer functional advantages to CAR-Vδ2 T cells remain to be identified.

RNA-seq analysis showed that ITGAE (CD103) was significantly upregulated in HPL-expanded CAR-Vδ2 T cells (supplemental figure S4B). CD103 is a key marker for tissue resident memory T cells (T_{RM}) upregulated by transforming growth factor β (TGF-β).[39,40] Peters et al. have reported CD103 upregulation in TGF-β-cultured Vδ2 T cells[41], and also documented downregulation of CD56 with enhanced *in vitro* short-term cytotoxicity of TGF-β-cultured Vδ2 T cells.[42] In addition, Beatson et al. demonstrated that *ex vivo* expanded Vδ2 T cells in the presence of TGF-β exhibited similar gene signatures to those reported by Peters et al.[41] and enhanced *in vivo* anti-tumor activity compared to cells without TGF-β.[43] HPL-expanded CAR-Vδ2 T cells shared some characteristics found in TGF-β-cultured Vδ2 T cells such as downregulation of CD56 expression (Figure 1D), upregulation of genes including ITGAE, CCR7, KLF7, and downregulation of genes including PTGER2, SMAD3, KLF3 (supplemental figure S4B) consistent with the high levels of TGF-β in HPL.[44] Therefore, TGF-β may be a key factor in enhancing the *in vivo* anti-tumor effects of HPL-expanded CAR-Vδ2 T cells. The pleomorphic activities of TGF-β also lead to inhibition of telomerase activity and acceleration of cellular senescence in multiple cell types.[45,46] In addition, there are some critical differences between HPL-expanded Vδ2 T cells and TGF-β-cultured Vδ2 T cells such as unchanged memory phenotype and reduced IL-2/STAT5 signaling signature as well as enriched gene signature of TGF-β signaling within Top 20 HALLMARK in FBS-expanded Vδ2 T cells (supplemental figure S4C). Therefore, TGF-β alone is unlikely to account for the differences in Vδ2 T cell functionality we saw and additional factors in HPL likely contribute.

We and others have shown that manufacturing conditions and medium composition affect the function of CAR-αβT cells.[47] For *ex vivo* expansion of Vδ2 T cells, investigators have used strategies such as Zol, isopentenyl pyrophosphate (IPP), or bromohydrin pyrophosphate (BrHPP) addition to stimulate Vδ2 T cell fraction in the presence of IL-2, IL-12, IL-15 and/or IL-18 alone or in combination,[48,49] or with feeder cells[50]. Since most of these studies have focused on investigating *ex vivo* cell expansion, phenotype, and short-term *in vitro* functionality, it is still unknown what types of culture materials and methods have the potential to contribute to long-term *in vivo* functionality of Vδ2 T cells. Our data support the use of HPL, which has been exploited to generate therapeutic cells in good manufacturing practice (GMP) facilities for cell-based therapy, as a simple means of enhancing the *in vivo* functionality of *ex vivo* expanded CAR-Vδ2 T cells for clinical use. Additional optimization of manufacture process including type of stimulus, cytokines, and duration of culture periods of HPL-expanded CAR-Vδ2 T cells could further improve their *in vivo* functionality.

We demonstrated one way to increase *in vivo* persistence of CAR-Vδ2 T cells, although *in vivo* efficacy of CD19.CAR-Vδ2 T cells is still suboptimal compared with CD19.CAR-αβT cells as evidenced in previous studies. Since our strategy was to utilize HPL-containing culture medium, additional genetic modifications to further enhance efficacy of HPL-expanded CAR-Vδ2 T cells can be combined and will need to be investigated.

Supplementary Material

Refer to Web version on PubMed Central for supplementary material.

Acknowledgements

Human platelet lysate (HPL; nLiven PR™) was provided by Sexton Biotechnologies (BioLife Solutions Inc., Bothell, WA). The authors thank Srila Sen for editing the manuscript.

Funding

The study was supported by the National Cancer Institute (P50CA126752 and F99CA253757), Stand Up to Cancer Dream Team in T-cell Lymphoma, CPRIT (RP230391 and RP210158), and DLDCCC Barry Stephen Smith Memorial Pancreatic Cancer Research Pilot Award.

Declaration of competing interests

H.E.H. is a cofounder with equity in Allovir and Marker Therapeutics; has equity in Fresh Wind Biotechnologies, CoRegen, and March Biosciences; has served on advisory boards for Tessa Therapeutics, Marker Therapeutics, and Kiadis; has received research funding from Tessa Therapeutics and Kuur Therapeutics. M.K.B. is a cofounder with equity in Allovir, Marker Therapeutics, and March Biosciences; has served on advisory boards for Tessa Therapeutics, Marker Therapeutics, Allogene, Walking Fish, Turnstone Biologics, Tscan, Bluebird Bio, Adaptimmune Therapeutics, Adintus, Onkimure, Triumvira Immunologics, Allogene, Bellicum Pharmaceuticals, Memgen, LLC, and Coya; has received royalties from Takeda, Bellicum, and Maker Therapeutics; has stock with Turnstone, Allogene, Walking Fish, AlloVir, and Tscan. M.M is a cofounder of March Biosciences and serves on advisory boards for March Biosciences and NKILT Therapeutics.

Availability of data and material

RNA-seq data are available at GEO under accession number GSE247760. All other data generated for this study will be made available upon reasonable request to the corresponding author.

References

1. Gu S, Borowska MT, Boughter CT, et al. Butyrophilin3A proteins and Vγ9Vδ2 T cell activation. Seminars in cell & developmental biology 2018;84:65–74. [PubMed: 29471037]
2. Rigau M, Ostrouska S, Fulford TS, et al. Butyrophilin 2A1 is essential for phosphoantigen reactivity by γδ T cells. Science (New York, N.Y.) 2020;367:
3. Nedellec S, Bonneville M, and Scotet E. Human Vgamma9Vdelta2 T cells: from signals to functions. Seminars in immunology 2010;22:199–206. [PubMed: 20447835]
4. Hoeres T, Smetak M, Pretscher D, et al. Improving the Efficiency of Vγ9Vδ2 T-Cell Immunotherapy in Cancer. Frontiers in immunology 2018;9:800. [PubMed: 29725332]
5. Grey A. Intravenous zoledronate for osteoporosis: less might be more. Therapeutic advances in musculoskeletal disease 2016;8:119–123. [PubMed: 27493690]
6. Ma L, Feng Y, and Zhou Z. A close look at current γδ T-cell immunotherapy. Frontiers in immunology 2023;14:1140623.
7. Mensurado S, Blanco-Domínguez R, and Silva-Santos B. The emerging roles of γδ T cells in cancer immunotherapy. Nature reviews. Clinical oncology 2023;20:178–191.
8. Torres Chavez A, McKenna MK, Canestrari E, et al. Expanding CAR T cells in human platelet lysate renders T cells with in vivo longevity. Journal for immunotherapy of cancer 2019;7:330. [PubMed: 31779709]
9. Watanabe N, and McKenna MK Generation of CAR T-cells using γ-retroviral vector. Methods in cell biology 2022;167:171–183. [PubMed: 35152995]

10. Subramanian A, Tamayo P, Mootha VK, et al. Gene set enrichment analysis: a knowledge-based approach for interpreting genome-wide expression profiles. Proceedings of the National Academy of Sciences of the United States of America 2005;102:15545–15550. [PubMed: 16199517]
11. Mootha VK, Lindgren CM, Eriksson KF, et al. PGC-1alpha-responsive genes involved in oxidative phosphorylation are coordinately downregulated in human diabetes. Nature genetics 2003;34:267–273. [PubMed: 12808457]
12. Liberzon A, Subramanian A, Pinchback R, et al. Molecular signatures database (MSigDB) 3.0. Bioinformatics (Oxford, England) 2011;27:1739–1740. [PubMed: 21546393]
13. Liberzon A, Birger C, Thorvaldsdóttir H, et al. The Molecular Signatures Database (MSigDB) hallmark gene set collection. Cell systems 2015;1:417–425. [PubMed: 26771021]
14. Park JH, and Lee HK Function of γδ T cells in tumor immunology and their application to cancer therapy. Experimental & molecular medicine 2021;53:318–327. [PubMed: 33707742]
15. Ito T, Teo YV, Evans SA, et al. Regulation of Cellular Senescence by Polycomb Chromatin Modifiers through Distinct DNA Damage- and Histone Methylation-Dependent Pathways. Cell reports 2018;22:3480–3492. [PubMed: 29590617]
16. Adams PD Remodeling of chromatin structure in senescent cells and its potential impact on tumor suppression and aging. Gene 2007;397:84–93. [PubMed: 17544228]
17. Kumari R, and Jat P. Mechanisms of Cellular Senescence: Cell Cycle Arrest and Senescence Associated Secretory Phenotype. Frontiers in cell and developmental biology 2021;9:645593.
18. Ganapathy T, Radhakrishnan R, Sakshi S, et al. CAR γδ T cells for cancer immunotherapy. Is the field more yellow than green? Cancer immunology, immunotherapy : CII 2023;72:277–286. [PubMed: 35960333]
19. Fisher J, Abramowski P, Wisidagamage Don ND, et al. Avoidance of On-Target Off-Tumor Activation Using a Co-stimulation-Only Chimeric Antigen Receptor. Molecular therapy : the journal of the American Society of Gene Therapy 2017;25:1234–1247. [PubMed: 28341563]
20. Huang SW, Pan CM, Lin YC, et al. BiTE-Secreting CAR-γδT as a Dual Targeting Strategy for the Treatment of Solid Tumors. Advanced science (Weinheim, Baden-Wurttemberg, Germany) 2023;10:e2206856.
21. Becker SA, Petrich BG, Yu B, et al. Enhancing the effectiveness of γδ T cells by mRNA transfection of chimeric antigen receptors or bispecific T cell engagers. Molecular therapy oncolytics 2023;29:145–157. [PubMed: 37387794]
22. Deniger DC, Switzer K, Mi T, et al. Bispecific T-cells expressing polyclonal repertoire of endogenous γδ T-cell receptors and introduced CD19-specific chimeric antigen receptor. Molecular therapy : the journal of the American Society of Gene Therapy 2013;21:638–647. [PubMed: 23295945]
23. Deniger DC, Maiti SN, Mi T, et al. Activating and propagating polyclonal gamma delta T cells with broad specificity for malignancies. Clinical cancer research : an official journal of the American Association for Cancer Research 2014;20:5708–5719. [PubMed: 24833662]
24. de Weerdt I, Lameris R, Scheffer GL, et al. A Bispecific Antibody Antagonizes Prosurvival CD40 Signaling and Promotes Vγ9Vδ2 T cell-Mediated Antitumor Responses in Human B-cell Malignancies. Cancer immunology research 2021;9:50–61. [PubMed: 33177109]
25. King LA, Toffoli EC, Veth M, et al. A bispecific γδ T-cell engager targeting EGFR activates a potent Vγ9Vδ2 T cell-mediated immune response against EGFR-expressing tumors. Cancer immunology research 2023;
26. Man F, Lim L, Volpe A, et al. In Vivo PET Tracking of (89)Zr-Labeled Vγ9Vδ2 T Cells to Mouse Xenograft Breast Tumors Activated with Liposomal Alendronate. Molecular therapy : the journal of the American Society of Gene Therapy 2019;27:219–229. [PubMed: 30429045]
27. Maude SL, Frey N, Shaw PA, et al. Chimeric antigen receptor T cells for sustained remissions in leukemia. The New England journal of medicine 2014;371:1507–1517. [PubMed: 25317870]
28. Porter DL, Hwang WT, Frey NV, et al. Chimeric antigen receptor T cells persist and induce sustained remissions in relapsed refractory chronic lymphocytic leukemia. Science translational medicine 2015;7:303ra139.

29. Kawalekar OU, O'Connor RS, Fraietta JA, et al. Distinct Signaling of Coreceptors Regulates Specific Metabolism Pathways and Impacts Memory Development in CAR T Cells. Immunity 2016;44:380–390. [PubMed: 26885860]
30. Salter AI, Ivey RG, Kennedy JJ, et al. Phosphoproteomic analysis of chimeric antigen receptor signaling reveals kinetic and quantitative differences that affect cell function. Science signaling 2018;11:
31. Xu W, and Larbi A. Markers of T Cell Senescence in Humans. International journal of molecular sciences 2017;18:
32. Bernadotte A, Mikhelson VM, and Spivak IM Markers of cellular senescence. Telomere shortening as a marker of cellular senescence. Aging 2016;8:3–11. [PubMed: 26805432]
33. Frisch SM, and MacFawn IP Type I interferons and related pathways in cell senescence. Aging cell 2020;19:e13234.
34. Lanna A, Coutavas E, Levati L, et al. IFN-α inhibits telomerase in human $CD8^+$ T cells by both hTERT downregulation and induction of p38 MAPK signaling. Journal of immunology (Baltimore, Md. : 1950) 2013;191:3744–3752. [PubMed: 23997212]
35. Kan CE, Cipriano R, and Jackson MW c-MYC functions as a molecular switch to alter the response of human mammary epithelial cells to oncostatin M. Cancer research 2011;71:6930–6939. [PubMed: 21975934]
36. Bryson BL, Junk DJ, Cipriano R, et al. STAT3-mediated SMAD3 activation underlies Oncostatin M-induced Senescence. Cell cycle (Georgetown, Tex.) 2017;16:319–334. [PubMed: 27892764]
37. Zheng L, Fisher G, Miller RE, et al. Induction of apoptosis in mature T cells by tumour necrosis factor. Nature 1995;377:348–351. [PubMed: 7566090]
38. Roberts AI, Devadas S, Zhang X, et al. The role of activation-induced cell death in the differentiation of T-helper-cell subsets. Immunologic research 2003;28:285–293. [PubMed: 14713720]
39. Zhang N, and Bevan MJ Transforming growth factor-β signaling controls the formation and maintenance of gut-resident memory T cells by regulating migration and retention. Immunity 2013;39:687–696. [PubMed: 24076049]
40. Qiu Z, Chu TH, and Sheridan BS TGF-β: Many Paths to CD103(+) CD8 T Cell Residency. Cells 2021;10:989. [PubMed: 33922441]
41. Peters C, Häsler R, Wesch D, et al. Human Vδ2 T cells are a major source of interleukin-9. Proceedings of the National Academy of Sciences of the United States of America 2016;113:12520–12525. [PubMed: 27791087]
42. Peters C, Meyer A, Kouakanou L, et al. TGF-β enhances the cytotoxic activity of Vδ2 T cells. Oncoimmunology 2019;8:e1522471.
43. Beatson RE, Parente-Pereira AC, Halim L, et al. TGF-β1 potentiates Vγ9Vδ2 T cell adoptive immunotherapy of cancer. Cell reports. Medicine 2021;2:100473.
44. Canestrari E, Steidinger HR, McSwain B, et al. Human Platelet Lysate Media Supplement Supports Lentiviral Transduction and Expansion of Human T Lymphocytes While Maintaining Memory Phenotype. Journal of immunology research 2019;2019:3616120.
45. Li H, Xu D, Li J, et al. Transforming growth factor beta suppresses human telomerase reverse transcriptase (hTERT) by Smad3 interactions with c-Myc and the hTERT gene. The Journal of biological chemistry 2006;281:25588–25600. [PubMed: 16785237]
46. Tominaga K, and Suzuki HI TGF-β Signaling in Cellular Senescence and Aging-Related Pathology. International journal of molecular sciences 2019;20:
47. Watanabe N, Mo F, and McKenna MK Impact of Manufacturing Procedures on CAR T Cell Functionality. Frontiers in immunology 2022;13:876339.
48. Yazdanifar M, Barbarito G, Bertaina A, et al. γδ T Cells: The Ideal Tool for Cancer Immunotherapy. Cells 2020;9:
49. Domae E, Hirai Y, Ikeo T, et al. Cytokine-mediated activation of human ex vivo-expanded Vγ9Vδ2 T cells. Oncotarget 2017;8:45928–45942. [PubMed: 28521284]
50. Xiao L, Chen C, Li Z, et al. Large-scale expansion of Vγ9Vδ2 T cells with engineered K562 feeder cells in G-Rex vessels and their use as chimeric antigen receptor-modified effector cells. Cytotherapy 2018;20:420–435. [PubMed: 29402645]

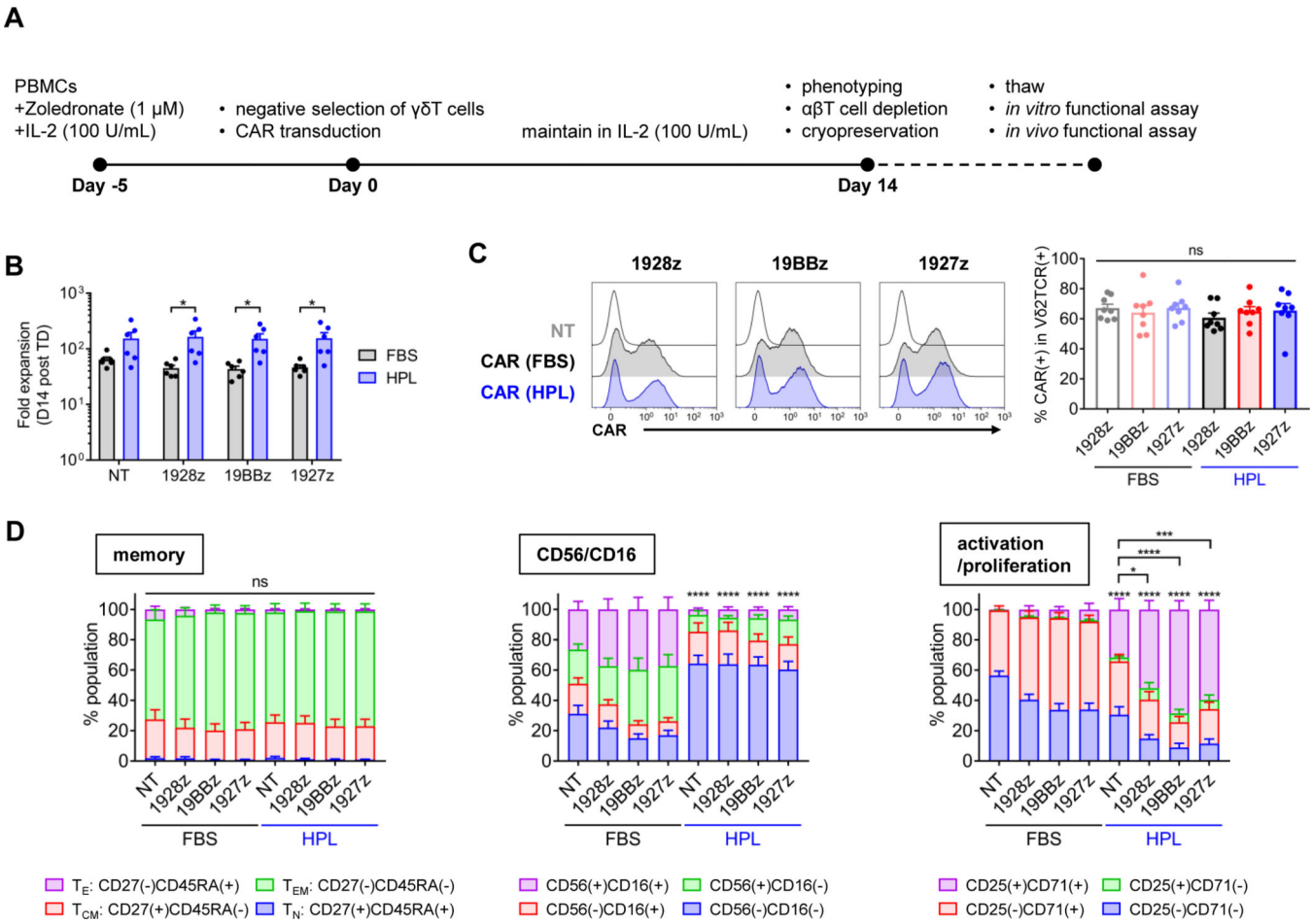

Figure 1. Expansion and surface phenotype of Vδ2 T cells generated in different media formulations

(A) A timeline of CAR-Vδ2 cell generation and overview of study design. (B) Total cell fold expansion on day 14 post transduction (mean ± S.E., n = 6). (C) Representative overlay histograms show CAR expression on Vδ2 T cells on day 14 post transduction (left), and the bar graph summarizes the results of multiple donors (right) (mean ± S.E., n = 8). (D) Surface phenotype of CAR-Vδ2 T cells on day 14 post transduction (mean ± S.E., n=8). Statistical differences are shown compared with FBS counterparts. Percentage of CD27(+)CD45RA(−), CD56(−)CD16(−) or CD25(+)CD71(+) is used for statistical analysis. Statistical differences are calculated by paired t test (B) or one-way ANOVA with Tukey multiple comparisons (C, D). *p < 0.05, **p < 0.01, ***p < 0.001, ****p < 0.0001, n.s, non-significant. PBMCs, peripheral blood mononuclear cells; CAR, chimeric antigen receptor; NT, non-transduced; 1928z, CD19.CAR with CD28z; 19BBz, CD19.CAR with 4–1BBz; 1927z, CD19.CAR with CD27z; FBS, fetal bovine serum; HPL, human platelet lysate; T_E, effector; T_{EM}, effector memory; T_{CM}, central memory; T_N, naïve.

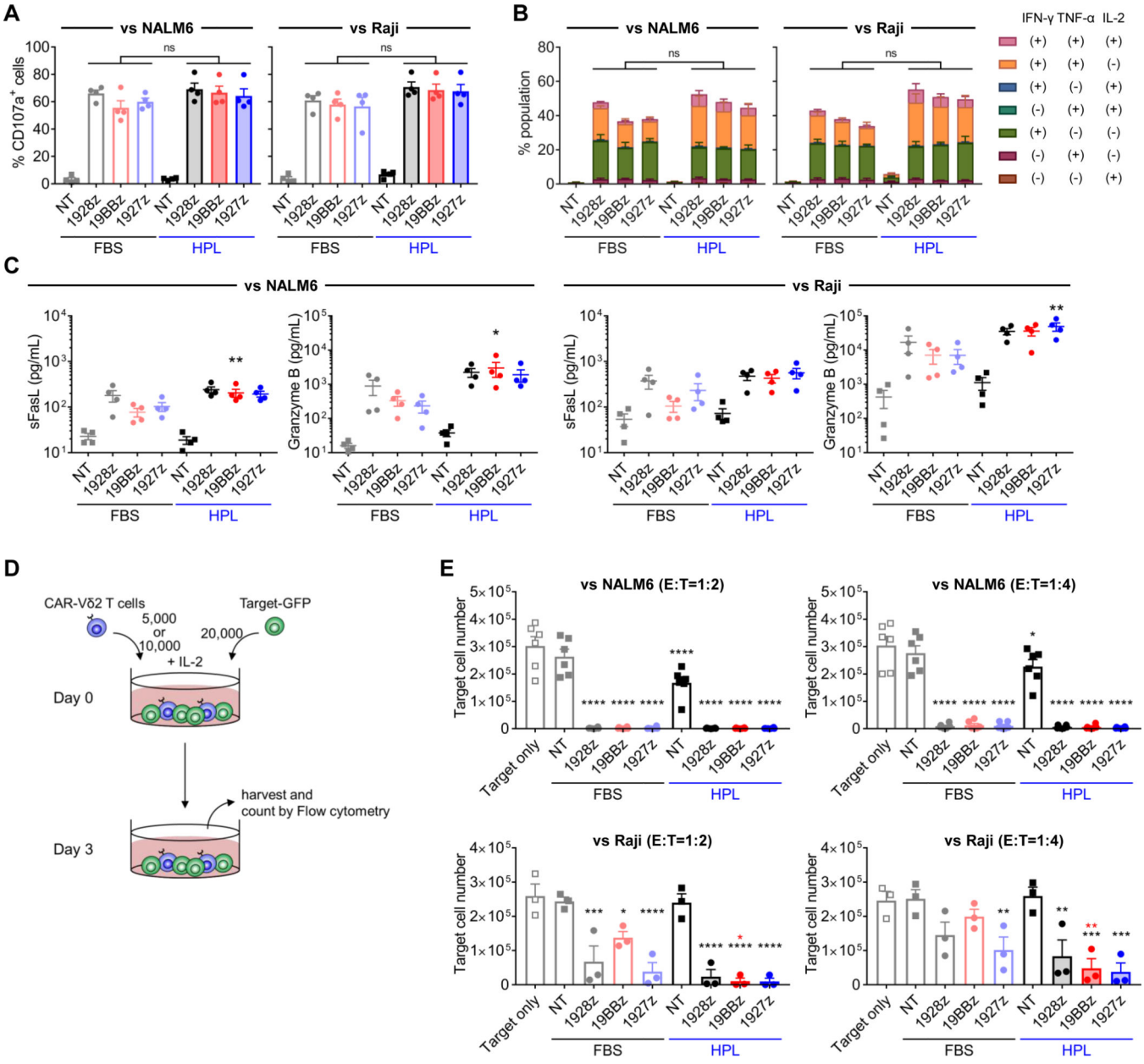

Figure 2. *In vitro* short-term functionality of CAR-Vδ2 T cells

(A, B) CD107a degranulation assay (A) and intracellular cytokine staining (B). CAR-Vδ2 T cells are cocultured with either NALM6 or Raji for 4 hrs (mean ± S.E., n = 4). (C) Soluble FasL and Granzyme B secretion from CAR-Vδ2 T cells. CAR-Vδ2 T cells are cocultured with either NALM6 (left) or Raji (right) for 24 hrs (mean ± S.E., n = 4). Statistical differences are shown compared with FBS counterparts. (D) Schematic of 3-day *in vitro* coculture setup. (E) Residual NALM6 (top) or Raji (bottom) cell numbers at 72 hrs after coculture with CAR-Vδ2 T cells at 1:2 (left) and 1:4 (right) effector-to-target ratios (mean ± S.E., n = 6). Statistical differences represented by black asterisks and red asterisks are shown between each cell type and Target only, and HPL and FBS, respectively. Statistical differences are calculated by one-way ANOVA with Tukey multiple comparisons

(A-C, E). *p < 0.05, **p < 0.01, ***p < 0.001, ****p < 0.0001, n.s, non-significant. NT, non-transduced; 1928z, CD19.CAR with CD28z; 19BBz, CD19.CAR with 4–1BBz; 1927z, CD19.CAR with CD27z; FBS, fetal bovine serum; HPL, human platelet lysate; CAR, chimeric antigen receptor; GFP, green fluorescent protein.

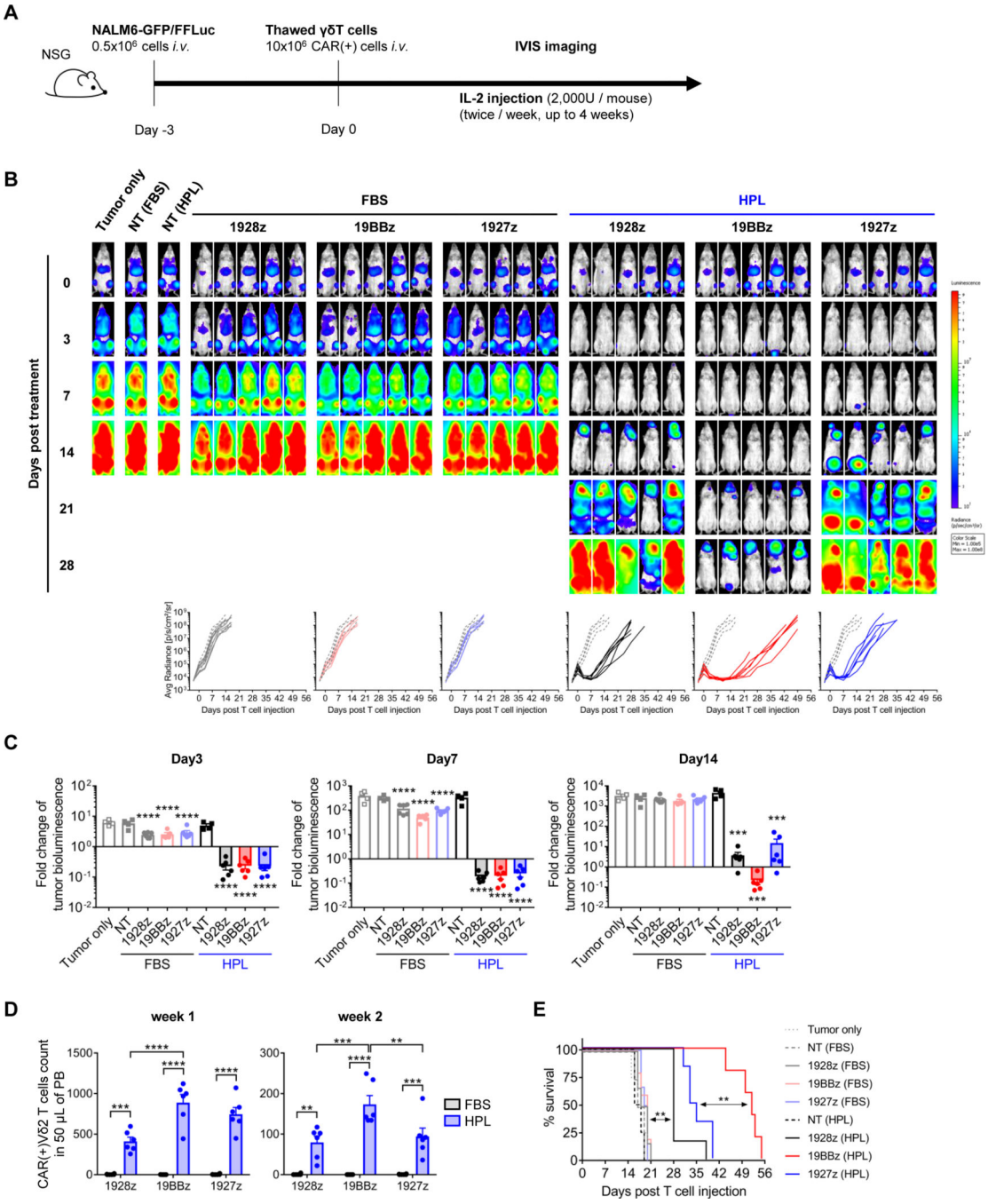

Figure 3. *In vivo* anti-tumor effect of CAR-Vδ2 T cells

(A) Schematic of *in vivo* experiment. (B) Representative mouse images show bioluminescence from tumor cells at different time points. Graph summarizes the results of bioluminescence from individual mice in each cell type group (n = 4–6 mice/group). Dotted lines and solid lines indicate tumor only group and treated group, respectively. (C) Fold change of tumor bioluminescence from day 0 at indicated time point (mean ± S.E., n = 4–6 mice/group). Statistical differences are shown between each cell type and Target only group. (D) Absolute count of CAR(+)Vδ2TCR(+) T cells in 50 μL of mouse peripheral blood on

week 1 and week 2 post T cell injection (mean ± S.E., n = 6 mice/group). (E) Animal survival over time. Statistical differences are calculated by one-way ANOVA with Tukey multiple comparisons (C, D) or log rank test (E). **p < 0.01, ***p < 0.001, ****p < 0.0001. GFP, green fluorescent protein; FFLuc, firefly luciferase; *i.v.*, intravenous; CAR, chimeric antigen receptor; FBS, fetal bovine serum; HPL, human platelet lysate; NT, non-transduced; 1928z, CD19.CAR with CD28z; 19BBz, CD19.CAR with 4–1BBz; 1927z, CD19.CAR with CD27z; Avg Radiance, average radiance; PB, peripheral blood.

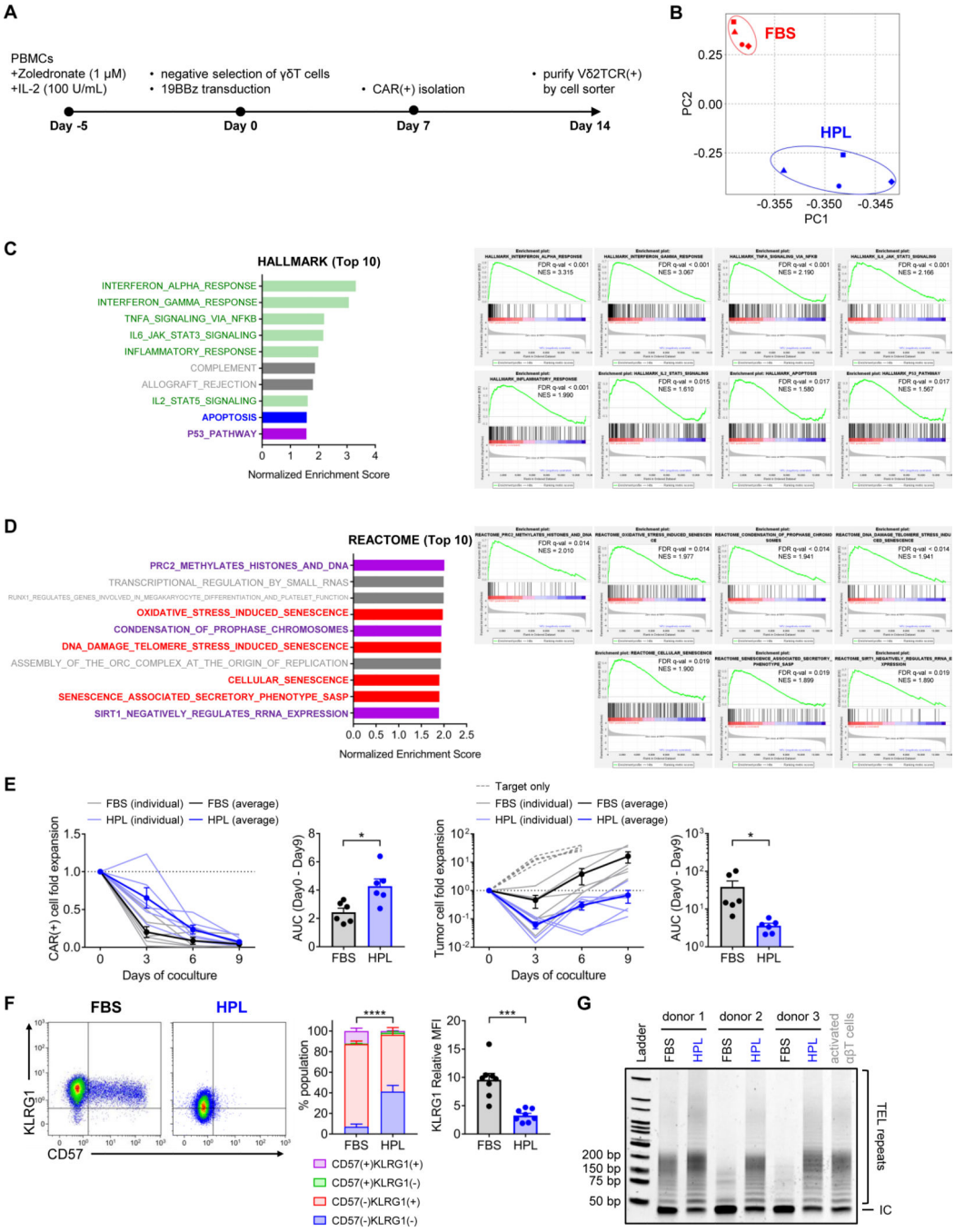

Figure 4. Distinct characteristics between CAR-Vδ2 T cells generated in different medium formulations

(A) An outline of CAR-Vδ2 T cell generation for RNA sequencing. (B) Principal component analysis of transcripts from FBS- and HPL-expanded CAR-Vδ2 T cells. (C, D) Gene set enrichment analysis with HALLMARK and REACTOME molecular signatures database. Top 10 gene set ranked by FDR is listed with normalized enrichment score (left) and the enrichment plot of selected gene sets (right) are shown. (E) Long-term *in vitro* coculture experiment. CD19.CAR (BBz)-Vδ2 T cells generated in FBS- and HPL-supplemented medium are cocultured with NALM6 at 1:2 effector-to-target ratio without

exogenous IL-2. Fold expansion of CAR(+) cells (left) and tumor cells (right) are shown. In the line graph, light blue and light black lines indicate data from individual donors in HPL and FBS conditions, respectively. Bold blue and bold black lines indicate averages of all donors in HPL and FBS conditions (mean ± S.E., n = 6). Dotted line indicates target only condition. The bar graph shows area under the curve (AUC) calculated in the line graph. (F) Representative flow plots show CD57 and KLRG1 expression on CAR-Vδ2 T cells. Bar graphs summarize the result of multiple donors (mean ± S.E., n = 8). Percentage of CD57(−)KLRG1(−) is used for statistical analysis in the stacked bar graph. (G) Gel image shows the result of telomeric repeat amplification protocol (TRAP). CAR-Vδ2 T cells were generated in FBS- or HPL-supplemented medium from three different donors and subjected to TRAP assay. TEL repeats; telomeric repeats. IC; internal control. Statistical differences are calculated by paired t test (E, F). *$p < 0.05$, ***$p < 0.001$, ****$p < 0.0001$. PBMCs, peripheral blood mononuclear cells; 19BBz, CD19.CAR with 4–1BBz; CAR, chimeric antigen receptor; FBS, fetal bovine serum; HPL, human platelet lysate; PC, principal component; FDR, false discovery rate; NES, normalized enrichment score; AUC, area under curve; TEL repeats, telomeric repeats; IC, internal control.

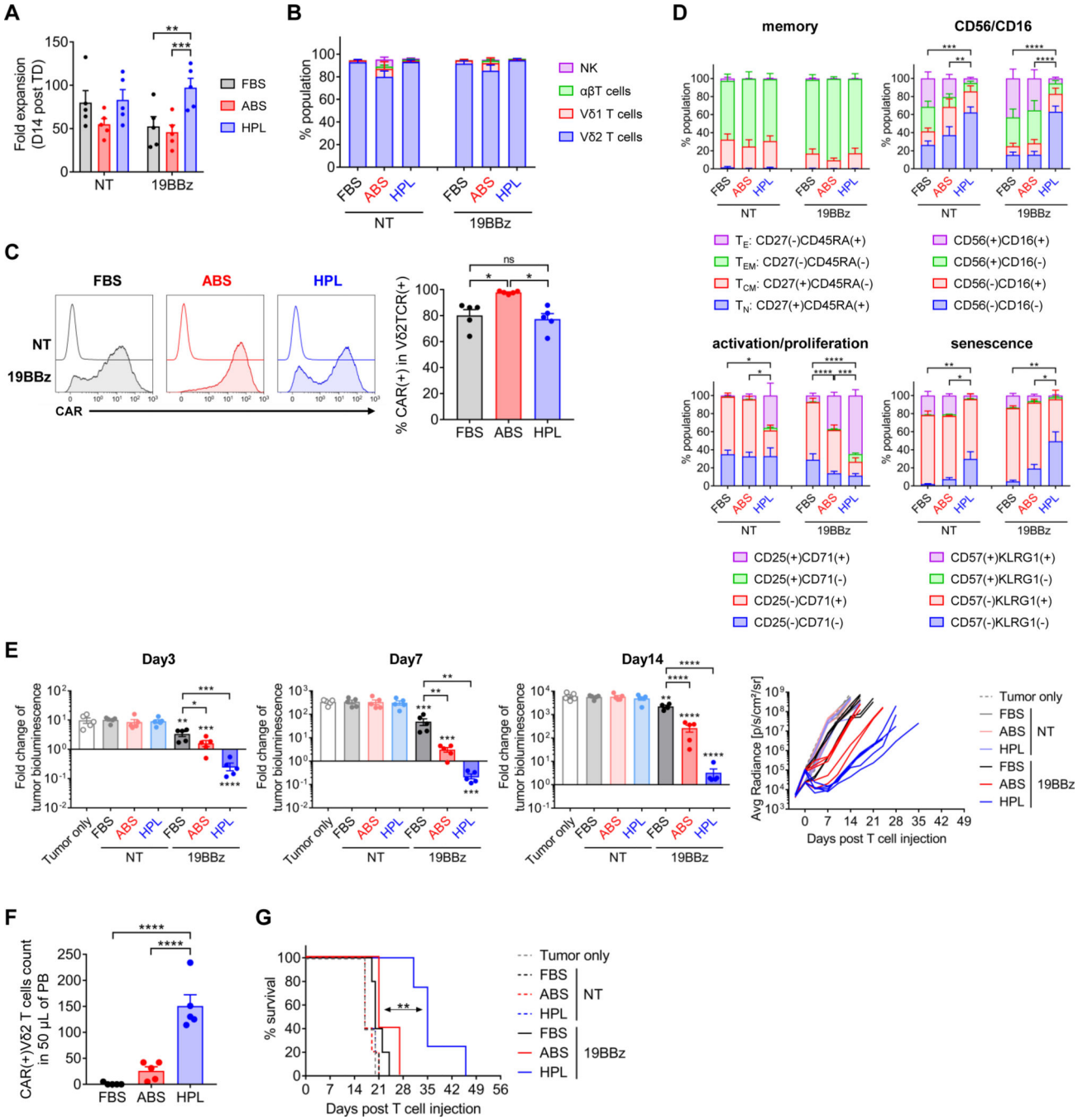

Figure 5. HPL-manufactured CAR-Vδ2 T cells outperformed FBS- and ABS-manufactured CAR-Vδ2 T cells

(A) Total cell fold expansion on day 14 post transduction (mean ± S.E., n = 5). (B) Cell population distribution on day 14 post transduction (mean ± S.E., n = 5). (C) Representative overlay histograms show CAR expression on Vδ2 T cells on day 14 post transduction (left), and the bar graph summarizes the results of multiple donors (right) (mean ± S.E., n = 5). (D) Surface phenotypes of CAR-Vδ2 T cells on day 14 post transduction (mean ± S.E., n=5). Percentage of CD27(+)CD45RA(−), CD56(−)CD16(−), CD25(+)CD71(+) or CD57(−)KLRG1(−) is used for statistical analysis. (E) Fold change

of tumor bioluminescence from day 0 at indicated time points (mean ± S.E., n = 5 mice/treatment group) and overall tumor growth over time. Statistical differences are shown between each cell type and tumor only, unless otherwise indicated. (F) Absolute count of CAR(+)Vδ2TCR(+) T cells in 50 μL of mouse peripheral blood on week 1 post T cell injection (mean ± S.E., n = 5 mice/group). (G) Animal survival over time. Statistical differences are calculated by one-way ANOVA with Tukey multiple comparisons (A-F) or log rank test (G). *$p < 0.05$, **$p < 0.01$, ***$p < 0.001$, ****$p < 0.0001$, n.s, non-significant. NT, non-transduced; 19BBz, CD19.CAR with 4–1BBz; FBS, fetal bovine serum; ABS, human AB serum; HPL, human platelet lysate; T_E, effector; T_{EM}, effector memory; T_{CM}, central memory; T_N, naïve; Avg Radiance, average radiance; PB, peripheral blood.